Catalysis Letters, Vol. 117, Nos. 1–2, August 2007 (© 2007)
DOI: 10.1007/s10562-007-9110-0

Catalytic oxidation of cyclopentene to glutaraldehyde over WO_3/Ti–HMS catalyst

Zhiqing Zhu,* Wei Bian, Longsheng Liu, and Zihong Lü

Institute of Chemical Engineering, East China University of Science and Technology, Shanghai 200237, PR China

Received 24 March 2007; accepted 31 March 2007

The high yield of 81% for the heterogeneous catalytic oxidation of cyclopentene with 50% aqueous hydrogen peroxide solutions to glutaraldehyde over WO_3/Ti–HMS catalyst was obtained. Based on characterizations such as: X-ray diffraction, surface area determination and potentiometric titration measurements, the activity and selectivity of WO_3/Ti–HMS catalyst were effectively attributed to a high amorphous WO_3 loading, as well as an appropriate structure of Ti–HMS support.

KEY WORDS: cyclopentene; glutaraldehyde; Ti–HMS; WO_3/Ti–HMS.

1. Introduction

Glutaraldehyde has been used extensively for disinfecting and sterilizing in many areas. However, the complicated preparation process and expensive materials restrict the commercial production from propenal [1,2]. The selective oxidation of cyclopentene with aqueous hydrogen peroxide solutions is a conducive pathway for producing glutaraldehyde [3,4]. This is due to the large quantity of cyclopentene, which is easily obtained from the by-products of five-carbon fractions presented in refining oils. Various tungsten-containing homogeneous catalysts have been found efficient for selectively oxidizing cyclopentene into glutaraldehyde. However, it is difficult to separate and recover the catalysts from the reaction mixture [5,6]. Recently, a number of W-containing heterogeneous catalysts, such as WO_3/TiO_2–SiO_2, W-MCM41, WO_3/HMS and W–HMS, were prepared and evaluated with a selectivity of 75% to glutaraldehyde and a high conversion of cyclopentene [7–11]. The oxidation of cyclopentene over these heterogeneous catalysts would take more than 20 h to reach the complete conversion of cyclopentene. It has been found that they are not efficient enough for industrial applications. Therefore, we propose an increase of amorphous WO_3 loading on the catalyst to improve the catalytic activity. This played an important role in determining the performance of catalyst. In order to increase the catalytic activity, a method of improving the porosity of supports was also suggested [7–11].

Studies on WO_3-based heterogeneous catalyst deposited on the titanium-containing hexagonal mesoporous silica (Ti–HMS) were carried out for selectively oxidizing cyclopentene. WO_3/Ti–HMS showed excellent activity and selectivity for producing glutaraldehyde. The results were superior to those previously reported [7–11]. The effects of various factors on the catalytic activity and selectivity are also discussed in this paper.

*To whom correspondence should be addressed.
E-mail: zhuzq@ecust.edu.cn

2. Experimental

The titanium containing HMS molecular sieve with a Si/Ti atomic ratio of 40 was synthesized by the gel method [12]. All catalysts were prepared by impregnating the Ti–HMS support with ($(NH_4)_2WO_4$) as follows: 0.6 g of $(NH_4)_2WO_4$ was dissolved in a solution of oxalic acid at the temperature of 353 K. A weight amount of Ti–HMS varied to obtain different WO_3-loadings was mixed homogenously into the solution. After being kept at ambient temperature for 20 h, the paste was dried in the oven at 293 K for 2 h, followed by calcination at 573 K in air for another 2 h.

Low and wide-angle X-ray powder diffraction patterns were recorded on Rigaku D/MAX-2500 spectrometer with Cu K_α radiation. The instrument was operated at 60 mA and 40 kV. The specific surface areas and the mean pore diameters of samples were measured and calculated according to the BET method with a Micromeritics Tri Star ASAP 2010 BET spectrometer with liquid nitrogen at 77 K. The acidity of the catalyst was measured by potentiometric titration analysis. A small quantity of 0.05 g solid sample was suspended in distilled water at 323 K, agitating for 2 h. The suspension was titrated with 0.03 N KOH solution at 0.01 mL min^{-1}. The electrode potential variation was registered on an ORIO-818 digital pH meter. The mass of the solid and the quantity of base used to reach equilibrium depend on the acidity of the sample solid.

The reproducibility of the electrode potential curve was ± 3 mV.

In a typical run, the oxidation reaction was carried out in a sealed 100 ml reactor in which 14 mL of 50% aqueous H_2O_2 solution (industrial grade), 60 mL of tert-butyl alcohol as the solvent, and 2.0 g catalyst were mixed. Afterward, 10 mL of cyclopentene was added via a dropping funnel under vigorous stirring and was allowed to react at 308 K for 8 h. The products of the oxidation of cyclopentene were analyzed on a gas chromatograph (GC-9800) equipped with a 0.32 mm $\times$ 30 m capillary column (FFAP) and a FID detector. An internal standard method was used to precisely calculate the content of glutaraldehyde in the oxidation products. The catalyst-recycling test was carried out as follows: The sedimentary catalyst was carefully recovered from the reaction solution by filtration. Then, the recovered catalyst was charged in the reactor together with the new reactant and solvent, followed by a subsequent reaction at the conditions mentioned above. After separation, the clear reaction solution sample was analyzed for titanium and tungsten-leaching ions with ICP-AES IRIS1000.

3. Results and discussion

3.1. X-ray diffraction

The low angle XRD patterns of Ti-HMS support and WO_3/Ti–HMS catalysts were shown in figure 1. Except for the 40% WO_3/Ti–HMS, the samples exhibite an intense diffraction peak corresponding to the (100) plane at 2θ of 2–3°, which is a typical characteristic of HMS materials. However, the intensity of the reflection decreases and the d_{100} spacing broadens with the increase of the WO_3-loading, which suggests a decrease in uniformity of the porous structure. Compared with the curves (d–f) in figure 1, the diffraction peaks corresponding to the (100) plane do not change obviously. It indicates that the porous structure of the catalyst does not collapse during the reaction and regeneration processes.

From the Wide-angle XRD patterns as shown in figure 2, no peaks corresponding to crystalline WO_3 are observed in the catalyst with WO_3-loading below 30 wt.%, which indicates the absence of agglomerated crystalline WO_3 in the samples. The strong characteristic peaks of crystalline WO_3 appears when the WO_3-loading reaches 40 wt%, suggesting that WO_3 begins to congregate on the surface of Ti–HMS. Others [8–11] reported that WO_3 began to congregate at WO_3-loading less than 20 wt.% when it was supported on pure silica molecular sieves. Wachs et al. [13] investigated the structures of tungsten oxide catalyst and found that more WO_3 could be dispersed on the surface of TiO_2 than that of SiO_2. In our experiments, by introducing Ti^{4+} into HMS, the porosity configuration and WO_3-loading amount are significantly improved so that more WO_3 can be dispersed on the surface of Ti–HMS. It is noted that the crystalline WO_3 disappears for the re-used catalyst regenerated by calcination at high temperatures, suggesting the re-dispersion of tungsten species under these regeneration conditions.

3.2. BET surface and pore diameter

The porosity configuration of the Ti-HMS and WO_3/Ti–HMS sample was measured by BET method. As shown in figure 3, the nitrogen adsorption isotherms have the shape of the type IV isotherm according to the IUPAC classification, with a sharp step at intermediate relative pressures, which indicates that the materials possess regular mesopores. Nitrogen isotherms exhibit

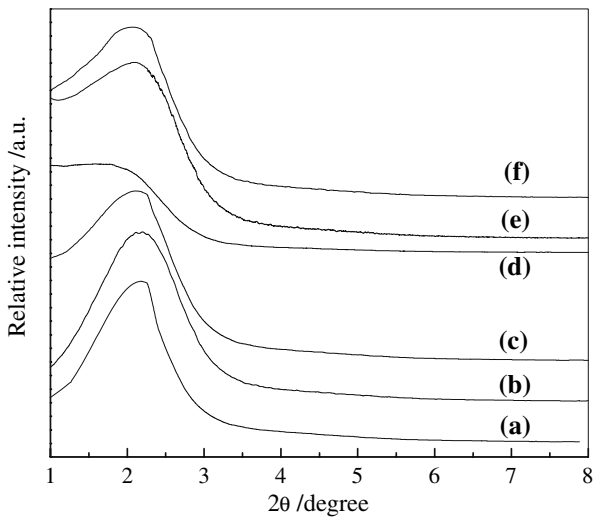

Figure 1. Small-XRD patterns of WO_3/Ti–HMS with different WO_3-loading (wt%): (a) 0%, (b) 20%, (c) 30%, (d) 40%, (e) 30%, after five reaction cycles, (f) 30%, calcined at 573 K after five reaction cycles.

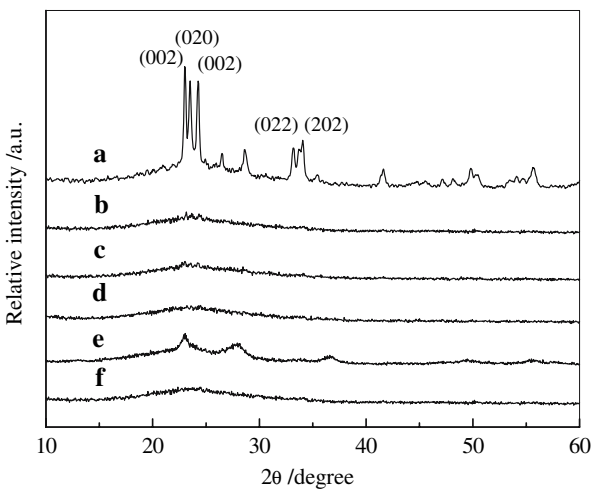

Figure 2. XRD patterns of WO_3/Ti–HMS with different WO_3-loading (wt%): (a) 40%, (b) 30%, (c) 20%, (d) 0%, (e) 30%, after five reaction cycles, (f) 30%, calcined at 573 K after five reaction cycles.

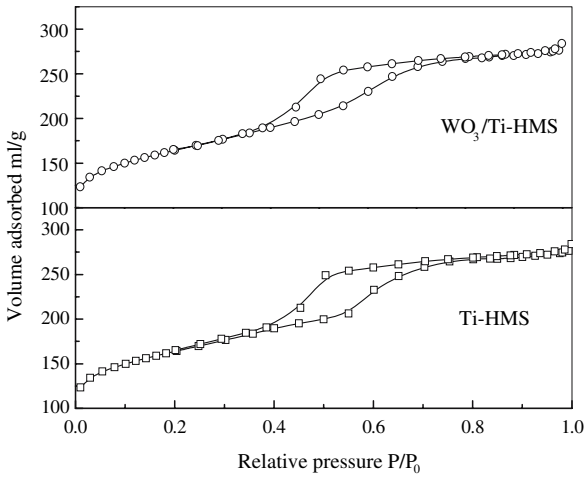

Figure 3. N_2 isotherms for WO_3/Ti–HMS (30 wt%) and Ti–HMS.

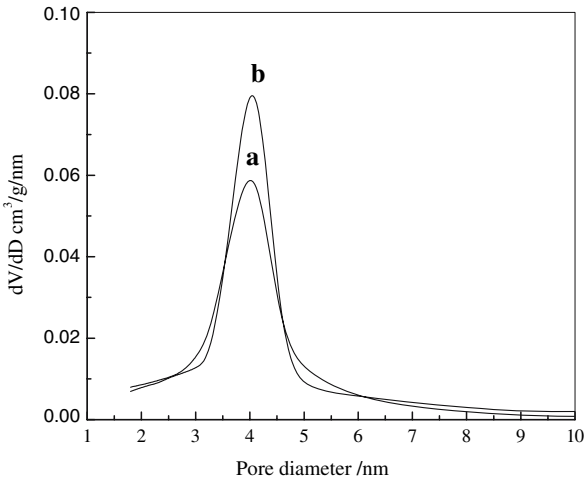

Figure 4. Pore size distribution for (a) WO_3/Ti–HMS (30 wt%) and (b) Ti–HMS.

hysteresis loops, probably because of the condensation within interparticle spaces. The calculated data of surface area and pore diameter are presented in table 1. It was found that as the pore diameter increased the BET surface area decreased for Ti-HMS supports compared with that of HMS. This may be attributed to the incorporation of titanium into the silicon framework. However, the BET surface area and pore volume decreased further after the impregnation process. It can be explained by two reasons. First, the addition of tungsten increases the density of the sample. Second, some tungsten species have diffused into the pores. From figure 4, both Ti–HMS and WO_3/Ti–HMS samples have a single distribution peak of pore size. The peak of pore size distribution of WO_3/Ti–HMS becomes wider than that of Ti–HMS, resulting from the impregnation of WO_3.

3.3. Potentiometric titration analysis

A potentiometric method was used to measure the number and strength of acid sites in a solid sample. The protocol of the method was briefly reported by Goldstein [14] and by Ruby [15]. The titration curves obtained from the WO_3/Ti–HMS system are shown in figure 5. From the consumption of KOH, the quantity of acid was calculated as listed in table 2. Meanwhile, the highest potential value corresponded to the acid strength presented as mV. Based on the results presented in table 2, it was found that the quantity of acid and the acid strength varied with different WO_3-loading. The quantity of acid for WO_3/Ti–HMS catalyst increased with increasing WO_3-loading in the range of 0 wt% to 30 wt%, but decreased at WO_3-loading up to 40 wt%. The acid strength distributions as presented in figure 6 were obtained from the slope of potentiometric titration curve (figure 5) calculated following the differential of dN/dE. The large difference in acid strength between the five samples can be noted from the millivolt range. From WO_3-loading of 10–30 wt%, the differential curve of WO_3/Ti–HMS catalyst clearly showed two break points, which indicates there are two types of acid sites, weak and strong respectively. The pure Ti–HMS showed only one type of acid site at lower millivolt. Thus, the weaker one can be explained by the results from the groups on the surface of support, and the stronger one was generated from the tungsten oxide supported. In the case of WO_3-loading of 40 wt%, there was no obvious acid site on the WO_3/Ti–HMS. Considering the XRD patterns as presented in figure 2, it can be concluded that the crystallization of supported WO_3 was responsible for the changes in the total number of acid sites and their distribution.

3.4. Catalytic oxidation of cyclopentene

In our work we have studied the selective oxidation of cyclopentene to glutaraldehyde as shown in scheme 1 reported by Dai [16]. It can be seen from the reaction scheme that both cyclopentene oxide and β-hydroxylcyclopentyl hydroperoxide are intermediates from conversion

Table 1
Properties of various samples

Samples	WO_3-loading (wt%)	BET surface area (m^2g^{-1})	Pore diameter (nm)	Pore volume (cm^3g^{-1})
HMS	0	1140.0	2.8	1.07
Ti–HMS	0	981.5	4.2	0.93
WO_3/Ti–HMS	30	789.5	4.1	0.72

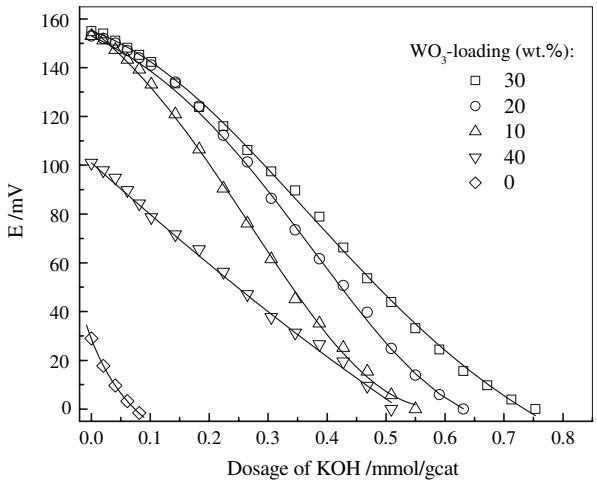

Figure 5. The titration curves for the WO_3/Ti–HMS catalysts.

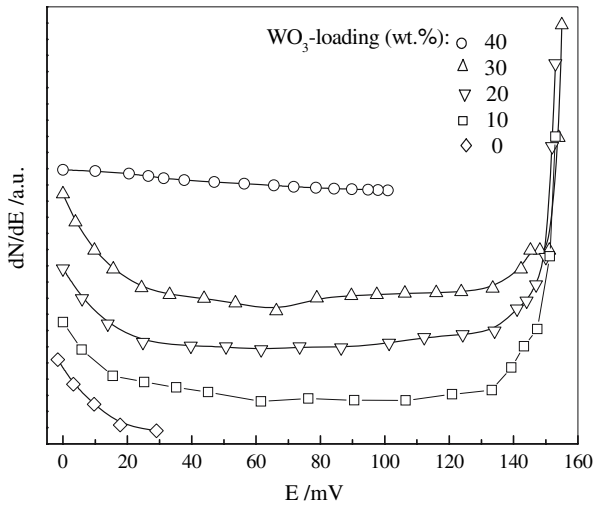

Figure 6. The acid strength distributions for the WO_3/Ti–HMS catalysts.

of cyclopentene to glutaraldehyde. Moreover, the parallel oxidation of cyclopentene oxide may occur to form the 1,2-cyclopentanediol (step 3). Side-products resulting from the etherification of cyclopentene oxide to form 2-butoxyl-1-cyclopentanediol could also be obtained (step 4) in the presence of tert-butyl alcohol as the solvent. Based on this scheme it can be inferred that the competitive reaction steps of cyclopentene oxide over heterogeneous catalysts govern the entire regioselective process.

3.4.1. *Effect of reaction time*

The distribution of products for the oxidation of cyclopentene over WO_3/Ti–HMS catalyst with WO_3-loading of 30 wt% is shown in figure 7. When the concentration of cyclopentene decreased to zero, the concentration of glutaraldehyde reached a plateau at reaction time of about 8 h. It proved that the activity of our catalyst was high, because the rate of reaction was faster than that of reactions carried out over other heterogeneous WO_3-containning catalyst [7–11]. The results obtained can be attributed to not only a higher quantity of WO_3-loading, but also the porosity configuration of the Ti–HMS support. The higher WO_3-loading is, the higher the acid strength and quantity of acid present, this also follows that there is a higher oxidation of cyclopentene and the process from intermediates to glutaraldehyde is faster. Moreover, the

Table 2
Acid character of WO_3/Ti–HMS catalysts with different WO_3-loading

WO_3-loading (wt%)	Acid strength (mV)	Quantity of acid (mmol $H_2WO_4g_{Cat}^{-1}$)
0	29	0.04
10	152	0.28
20	153	0.31
30	155	0.38
40	101	0.26

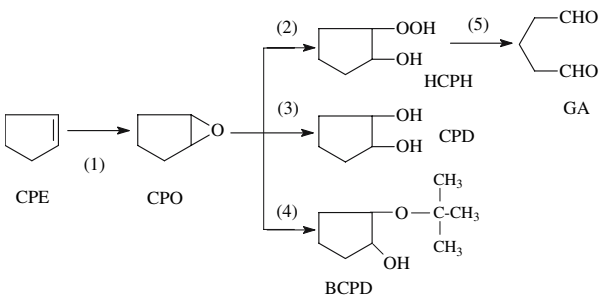

Scheme 1. Process of catalytic oxidation of cyclopentene CPE, cyclopentene; CPO, cyclopentene oxide; HCPH, β-hydroxylcyclopentyl hydroperoxide; CPD, 1,2-cyclopentanediol; BCPD, 2-butoxyl-1-cyclopentanediol; GA, glutaraldehyde.

Ti–HMS support is favorable to load more tungsten oxide that is active acid sites. Meanwhile, Ti–HMS supports also show the catalytic activity for the oxidation of alkene as reported in references [17,18]. It is possible that the interaction between WO_3 loaded and surface of the Ti–HMS affects the activity for the oxidation of cyclopentene. Therefore, it is reasonable to support that the catalyst transferred the active oxygen molecular from H_2O_2 to cyclopentene and catalyzed the reactions of steps 1, 2 and 5 [7–11, 16–18].

3.4.2. *Effect of WO_3 loading*

Results for oxidation of cyclopentene at reaction time of 8 h over WO_3/Ti–HMS catalyst prepared with different support and WO_3 content are reported in table 3. The performance of support Ti-HMS was evidently superior to HMS, showing the Ti element played an important role in this reaction to improve the activity and selectivity of the catalyst as discussed above. In the case of the supported catalysts, the effect of dispersion must be considered. Although the support of Ti-HMS without any loading WO_3 gives a conversion of 70.2%

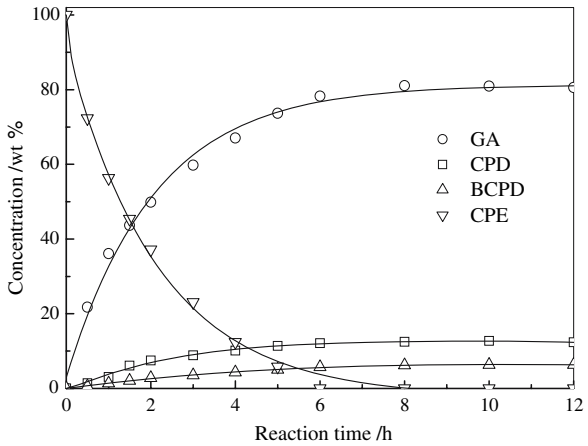

Figure 7. Distribution of products for the oxidation of cyclopentene over WO_3/Ti–HMS catalysts.

Table 3
Catalytic performance of catalysts with different support and WO_3-loading

WO_3 loading (wt%)	CPE conversion (%)		GA yield (%)	
	HMS	Ti–HMS	HMS	Ti–HMS
0	0	70.2	0	11.9
10	41.8	88.6	24.3	67.4
20	47.6	92.5	28.8	75.8
30	34.6	100.0	17.5	81.3
40	–	90.7	–	61.8

for cyclopentene, a yield of 11.9% for product glutaraldehyde is lower. However, a considerable amount of 1,2-cyclopentanediol was obtained, which was the by-product in the parallel oxidation pathway. This result showed that the WO_3 loaded is advantageous for the reaction to proceed towards the production of glutaraldehyde via reaction steps 2 and 3 as shown in scheme 1. This also showed that the stronger acid sites rather than the weaker one, shown in figure 6, are the main activity phase in this reaction system. Both the activity and selectivity of WO_3/Ti–HMS catalyst was increased with increasing the WO_3 loading below 30 wt%, but decreased while further increasing the WO_3 loading up to 40 wt%. The complete conversion of cyclopentene and a maximum yield of 81.3% for glutaraldehyde were obtained at WO_3 loading of 30 wt%. It is apparent that partial crystallization occurs when the WO_3-loading was up to 30 wt%, due to the gathering of the WO_3 species during the process of catalyst preparation. Therefore, the crystalline WO_3 was responsible for the decrease in catalytic activity and selectivity [11].

3.4.3. Durability of WO_3/Ti–HMS catalyst

Table 4 illustrates the durability of WO_3/Ti-HMS catalyst with WO_3 loading of 30 wt% at reaction time of 8 h. In all batch reactions, a high reaction conversion and a small decrease of yield was observed with catalyst cycle. However, the intrinsic catalytic activity could be recovered after calcination at 573 K in air for 4 h. In order to study the stability of the supported catalyst, the leaching of tungsten and titanium into the product mixture was also determined after every reaction cycle. As presented in table 4, the trace amount of tungsten and titanium detected in reaction solution revealed that both W and Ti species lost from the catalyst could be negligible. The XRD pattern for used and regenerated WO_3/Ti–HMS after five reaction cycles is shown in figure 2e and f, respectively. The weak peaks ascribed to crystalline WO_3 appeared for the used catalyst and disappeared after regeneration by treating at high temperature of 573 K. This result indicates that the congeries of tungsten species on the Ti–HMS during the reaction process might be responsible for the tendency of decreased activity.

4. Conclusions

In conclusion, crystal form, surface porosity and acidity of WO_3/Ti–HMS catalyst prepared by impregnation method were studied. The incorporation of titanium into the framework of HMS improved the dispersal of WO_3 leading to greater loading of amorphous WO_3 than the pure silicon supports. It was found that there were two types of acid sites on WO_3/Ti–HMS catalyst, the stronger one was the main activity phase. For the synthesis of glutaraldehyde from cyclopentene, WO_3/Ti–HMS catalyst with WO_3-loading of 30 wt%

Table 4
Catalyst recycle test

Run no.	CPE conversion (%)	GA yield (%)	Leached W (ppm)	Total lost W (wt.%)	Leached Ti (ppm)	Total lost Ti (wt.%)
1	100.0	81.3	51	0.2	11	1.7
2	100.0	80.5	76	0.5	6	2.6
3	100.0	78.5	204	1.3	5	3.4
4	98.7	76.2	281	2.4	7	4.3
5	93.5	68.8	306	3.6	4	4.9
6*	100.0	79.6	74	3.9	5	5.8

* After regeneration.

showed excellent activity and selectivity, and gave a high yield of 81.3% at reaction time of 8 h. The stability of titanium in the support and of active W-species on the catalyst was confirmed by the catalyst-recycling test of five cycles. Finally, the high activity of the catalyst could be regenerated by simple calcination.

References

[1] S.P. Gorman, E.M. Scott and A.D. Russell, J. Appl. Bacteriol. 48 (1980) 161.
[2] F.M. Collins, J. Appl. Bacteriol. 61(3) (1986) 247.
[3] W.J. Wang, M.H. Qiao, H.X. Li and J.F. Deng, Appl. Catal. A 166 (1998) 243.
[4] W.J. Wang, M.H. Qiao, H.X. Li, W.L. Dai and J.F. Deng, Appl. Catal. A 168 (1998) 151.
[5] J.F. Deng, X.H. Xu, H.Y. Chen and A.R. Jiang, Tetrahedron 48 (1992) 3503.
[6] X.H. Xu, H.Y. Chen, J.F. Deng and A.R. Jiang, Acta Chim. Sinica 53 (1993) 188.
[7] R.H. Jin, X. Xia, W.L. Dai, J.F. Deng and H.X. Li, Catal. Lett. 62 (1999) 201.
[8] H. Chen, W.L. Dai, J.F. Deng and K.N. Fan, Catal. Lett. 81 (2002) 131.
[9] W.L. Dai, H. Chen, Y. Cao, H.X. Li, S.H. Xie and K.N. Fan, Chem. Commun. 7 (2003) 892.
[10] X.L. Yang, W.L. Dai, J.H. Xu, H. Chen, Y. Cao and K.N. Fan, Chinese J. Catal. 4 (2005) 311.
[11] X.L. Yang, W.L. Dai, H. Chen, J.H. Xu, Y. Cao, H.X. Li and K.N. Fan, Appl. Catal. 283 (2005) 1.
[12] P.T. Tanev, M. Chibwe and T. Pinnavaia, Nature 267 (1994) 322.
[13] D.S. Kim, M. Ostromecki and I.E. Wachs, J. Mol. Catal. A 106 (1996) 93.
[14] M.S. Goldstein, in: *Experimental Methods in Catalytic Research*, R.B. Anderson (eds.(Academic Press, New York, 1968) pp. 361–361.
[15] C. Ruby and P. Gina, Appl. Catal. A 14 (1985) 15.
[16] W.L. Dai, X.J. Huang, H.Y. Chen and J.F. Deng, Indian J. Chem. 36B (1997) 583.
[17] O.A. Kholdeeva, A.Yu Derevyankin, A.N. Shmakov, N.N. Trukhan, E.A. Paukshtis, A. Tuel and V.N. Romannilov, J. Mol. Catal. A 158 (2000) 417.
[18] Z.H. Fu, D.L. Yin, Q.J. Xie, W. Zhao, A.X. Lv, D.H. Yin, Y.Z. Xu and L.X. Zhang, J. Mol. Catal. A 208 (2004) 159.